Supporting Information

Brusatte et al. 10.1073/pnas.0906911106

SI Text

Diagnosis and Justification of the New Species. Institute of Geology, Mongolia (IGM) 100/1844 is herein regarded as the holotype of a new species, *Alioramus altai*, which can be differentiated from other tyrannosaurids (most importantly the contemporary *Tarbosaurus* and the poorly understood Late Cretaceous *Alectrosaurus*) as well as the holotype of *Alioramus remotus*, the only other known specimen of the genus *Alioramus*.

IGM 100/1844 is clearly different from the contemporary *Tarbosaurus*, including juveniles of that genus. Several differences with juvenile *Tarbosaurus* are listed in the main text. There are several additional differences with specific exemplar specimens of juvenile *Tarbosaurus*. Institute of Palaeobiology, Warsaw, Poland (ZPAL) MgD-I/29 includes the skull and postcranial material of a juvenile *Tarbosaurus* of approximately the same skull size as the *A. altai* holotype. This specimen's maxilla is deeper than that of *A. altai* and is more convex anteriorly, unlike the elongate and low morphology of *A. altai*. The postorbital has a much larger and more prominent cornual process, and the ventral ramus does not taper (as in *A. altai*) but rather projects into the orbit as a sheet-like flange. The jugal lacks the autapomorphic lateral horn of *A. altai*. The fibular facet on the tibia is mostly anteriorly facing and does not face strongly laterally as in *A. altai*. The lateral malleolus of the tibia projects far laterally and distally, which is not the case in *A. altai*. ZPAL MgD-I/175 includes fragments of a juvenile *Tarbosaurus* skull, of approximately the same size as the *A. altai* holotype skull. The dentary has only 15 teeth and is deeper and more robust than that of *A. altai*, and the postorbital exhibits an orbital flange. ZPAL MgD-I/31 includes a surangular from a juvenile *Tarbosaurus*, which is almost exactly the same size as the surangulars in the *A. altai* holotype. It exhibits two important differences from *A. altai*: The muscular fossa above the surangular foramen faces mostly laterally (not dorsally), and there is no deep pocket behind the surangular fenestra.

IGM 100/1844 is also different from the possible Late Cretaceous (or early Late Cretaceous) *Alectrosaurus olseni*. Although similar in size, the hindlimb of the holotype of *A. altai* differs in many details from that of *A. olseni*. In the femur, the patellar sulcus is a deep cleft in the new taxon, whereas it is shallow in *A. olseni*; furthermore, the distal condyles are widely separated from each other in the new taxon, whereas they are narrowly separated in *A. olseni*. The contact between the tibia and the astragalus is different between the two species: whereas in the new taxon the medial margin of the ascending process extends vertically from its base before abruptly extending dorsolaterally, in *A. olseni* the angulation is absent and the entire margin extends at a steep dorsolateral angle. Furthermore, the pit at the base of the ascending process does not undercut the bone medial to it in the new taxon, whereas the pit undercuts the bone in *A. olseni*. The most distinct feature of the pes of *A. olseni*, in contrast to all other tyrannosauroids, including *A. altai*, is the hypertrophy of the distal joint surfaces of almost all of the metatarsals and pedal phalanges. In light of these differences, it is clear that IGM 100/1844 cannot be referred to *Alectrosaurus*, and we consider it justifiable to maintain generic separation of *Alectrosaurus* and *Alioramus*.

IGM 100/1844 and the holotype of *A. remotus* form a clade (herein referred to as the genus *Alioramus*) in our cladistic analysis (see *Phylogenetic Analysis*), which is supported by several characters elucidated in the main text. However, IGM 100/1844 also exhibits several differences with the holotype of *A. remotus*, which are listed in the main text. It is often difficult to determine whether such differences reflect taxonomic separation (i.e., are diagnostic of different species), or whether they are due to ontogenetic, sexual, or individual variation. This is especially difficult for *Alioramus*, as only two specimens are known, the holotype material of *A. remotus* is fragmentary, and the holotype material of *A. remotus* has only been briefly described and has largely been inaccessible to many researchers for several decades.

It is possible, in fact probable, that some of the differences between the two specimens are due to ontogeny. For example, the position of the anterior process of quadratojugal relative to the anterior margin of lateral temporal fenestra, position of the anterior process of the squamosal relative to the anterior margin of the lateral temporal fenestra, and bifurcation of the epipterygoid are all variable in *Tyrannosaurus rex*. However, keeping in mind that the holotype of *A. remotus* and IGM 100/1844 only differ in skull size by ≈3%, we consider it most reasonable to interpret many of these differences as taxonomic and most prudent to erect a new species (*A. altai*) for IGM 100/1844. It is important to consider this as a hypothesis, subject to testing by comparison with new specimens as they are discovered. With new discoveries, it is possible that *A. altai* may turn out to be the same as *A. remotus*. However, whether there are one or two species of *Alioramus*, this taxonomic conundrum does not take away from the main conclusion of the current paper, as revealed by the new specimen: that *Alioramus* is a derived tyrannosaurid that differs in size, skeletal proportions, and skull shape from its more familiar megapredatory cousins.

Skeletal Measurements of *A. altai*. Refer to Table S1, Table S2, and Table S3 for skeletal measurements.

Computed Tomography Scan. The braincase of the *A. altai* holotype (IGM 100/1844) was scanned on 21 January 2009 at The University of Texas High-Resolution X-ray Computed Tomography Facility, Austin. Scanning was performed by using a voltage of 450 kV and amperage of 3 mA. Scans were taken along the sagittal axis for a total of 431 slices at an image resolution of 1,024 × 1,024 pixels. The slice thickness and interslice spacing is 0.25 mm with a reconstructed field of view of 301.6 mm. Slices along the horizontal and coronal axes were reconstructed by G.S.B. by using VGStudioMax 1.2.1.

Histological Analysis. Diaphyseal, transverse plane histological thin sections of three major long bones were made and viewed with polarized microscopy. From these, the microstructure was described (1–5). Sectioned elements included the left fibula, left metatarsal IV, and a hindlimb stylopodial element (tibia, possible femur).

The majority of the cortex of the fibula is composed of primary fibro-lamellar bone. The deep cortex shows longitudinal vascularization. Nearer the midcortex, reticular and longitudinal vascularization are equally represented. Nearest the periosteal border, only longitudinal vascular canals are present. Some incompletely formed vascular canals were trapped at the periosteal surface at the time of death. A small medullary cavity lined by endosteal bone exists. Extensive, dense Haversian bone remodeling is found in the inner cortex. Nevertheless, remnants of nine growth lines in total, in the form of lines of arrested growth (LAGs) and a few annuli, are preserved throughout the element (common in fibulae from theropods; see ref. 3). This

finding made an estimate of longevity possible without the use of back-calculation techniques.

The majority of the metatarsal cortex is composed of dense Haversian tissue, whereas the outermost cortex shows primary bone (Fig. S1). The deepest regions of the latter show plexiform vascularization. The outermost section shows a mix of longitudinal and reticular vascular canals. The endosteal border of the element is scalloped from osteoclastic activity. The periosteal surface shows incompletely formed vascular canals like those seen in the fibula. Between three and four LAGs are found in the primary cortex. The last growth line is in the form of an annulus that is locally present (Note: The zones bounding it are well differentiated).

The stylopodial hindlimb element is entirely composed of primary bone that shows plexiform vascularization (Fig. S2). The endosteal border shows no lamellar bone. The periosteal border shows incompletely formed vascular canals like the other long bones. A single LAG is found very near the endosteal border of the bone.

The findings of (*i*) highly vascularized primary bone at the cortical surfaces of these elements, (*ii*) trapped primary vascular canals at the perioseal bone surfaces, (*iii*) signs of active resorption at the endosteal borders of two elements, (*iv*) growth zone spacing that does not diminish, and (*v*) intermediate Haversian bone formation (for a large tyrannosaur) all point to IGM 100/1844 as being a young, actively growing juvenile-to-subadult animal that died as a nine year old. Its size (based on femoral length) relative to age conforms most closely to *Gorgosaurus* and *Albertosaurus* (7–8 years old) versus expectations for larger taxa such as *Daspletosaurus* and *Tyrannosaurs* (5–6 years old) among North American tyrannosaurs (5). In fact, the greater age of this specimen in comparison with its former counterparts suggests a developmental trajectory consistent with an even smaller taxon.

Ontogeny Analysis. We provide the following block of data for *A. altai*, scored for the ontogenetic analysis of Carr and Williamson (6):
?????1100010001101010011000010100011000100100000000001-0011110000000000000000000000001?0.

This analysis returned a single most-parsimonious tree (99 steps; consistency index = 0.91; retention index = 0.91). The tree is shown in Fig. S3, with the arrow indicating increasing age toward the tip of the pectinate tree. Numbers next to nodes denote Bremer support/bootstrap (1,000 replications) values.

Phylogenetic Analysis: Data Matrix. The data matrix used to recover the phylogenetic position of *A. altai* among tyrannosauroids. *Coelophysis*, *Allosaurus*, *Velociraptor*, and *Sinosauropteryx* are outgroup taxa. For the character list and taxon scores for the phylogenetic analysis, please refer to the *SI Appendix*.

Phylogenetic Analysis: Inclusion of *Xiongguanlong*. The recently described basal tyrannosauroid *Xiongguanlong* possesses an elongate snout similar to that of *Alioramus*. However, the two are clearly distinct taxa: *Xiongguanlong* is smaller than *Alioramus*, possesses its own autapomorphies and lacks the autapomorphies of *Alioramus*, and lived more than 35 million years before *Alioramus*. We included *Xiongguanlong* in an earlier version of our cladistic analysis but do not depict its position in the cladogram in the main paper because it appears to act as a "wild card" taxon in the analysis. However, given the similar skull shapes of *Xiongguanlong* and *Alioramus*, we report our scores for *Xiongguanlong* below, and briefly discuss the impact of *Xiongguanlong* when it is included in the analysis.

Including *Xiongguanlong* results in two most-parsimonious trees (632 steps; CI = 0.60; RI = 0.64), the strict consensus of which finds an unresolved polytomy consisting of *Xionguanlong*, *Eotyrannus*, *Appalachiosaurus*, *Dryptosaurus*, and Tyrannosauridae. These results are consistent with previous analyses that show the position of those genera outside of Tyrannosauridae and confirms that *Xiongguanlong* and *Alioramus* are not particularly closely related taxa (i.e., *Xiongguanlong* is more basal than *Alioramus*). However, the position of the New Mexico taxon (7) is removed from its sister group position with Tyrannosauridae, and it is placed as the sister taxon of *Albertosaurus*. The relatively low number of characters (66 of 279) that could be scored for *Xiongguanlong* may in part have caused the conflict in the results. Therefore, this result is premature because of poor character sampling near the base of Tyrannosauroidea, an issue that will be addressed in the future.

1. Francillon-Vielliot H, et al. (1990) In *Biomineralization: Patterns and Evolutionary Trends*, ed Carter JG (Van Nostrand Reinhold, New York), pp 471–530.
2. Chinsamy A (2005) *The Microstructure of Dinosaur Bone: Deciphering Biology with Fine-Scale Techniques* (Johns Hopkins Press, Baltimore).
3. Erickson GM (2005) Assessing dinosaur growth patterns: A microscopic revolution. *Trends Ecol Evol* 20:677–684.
4. Sussman M (1964) *Growth and Development.* (Prentice-Hall, Englewood Cliffs, NJ).
5. Erickson GM, Makovicky PJ, Norell MA, Yerby SA, Brochu CA (2004) Gigantism and comparative life history parameters of tyrannosaurid dinosaurs. *Nature* 430:772–775.
6. Carr TD, Williamson TE (2004) Diversity of late Maastrichtian Tyrannosauridae (Dinosauria: Theropoda) from western North America. *Zool J Linn Soc* 142:479–523.
7. Carr TD, Williamson TE, A new tyrannosauroid from New Mexico and the origin of deep snouts in Tyrannosauroidea. *J Vertebr Paleontol*, in press.

Fig. S1. Diaphyseal metatarsal histology of IGM 100/1844. Arrows denote growth lines. The outermost line is variably present as an annulus that exists between two conspicuous growth zones (top arrow). Note the incompletely formed primary vascular canals (pitting) at the periosteal border of the element and how the growth zones do not show appreciably diminishing widths nearer the periosteal border of the element. (Scale bar, 0.5 mm.)

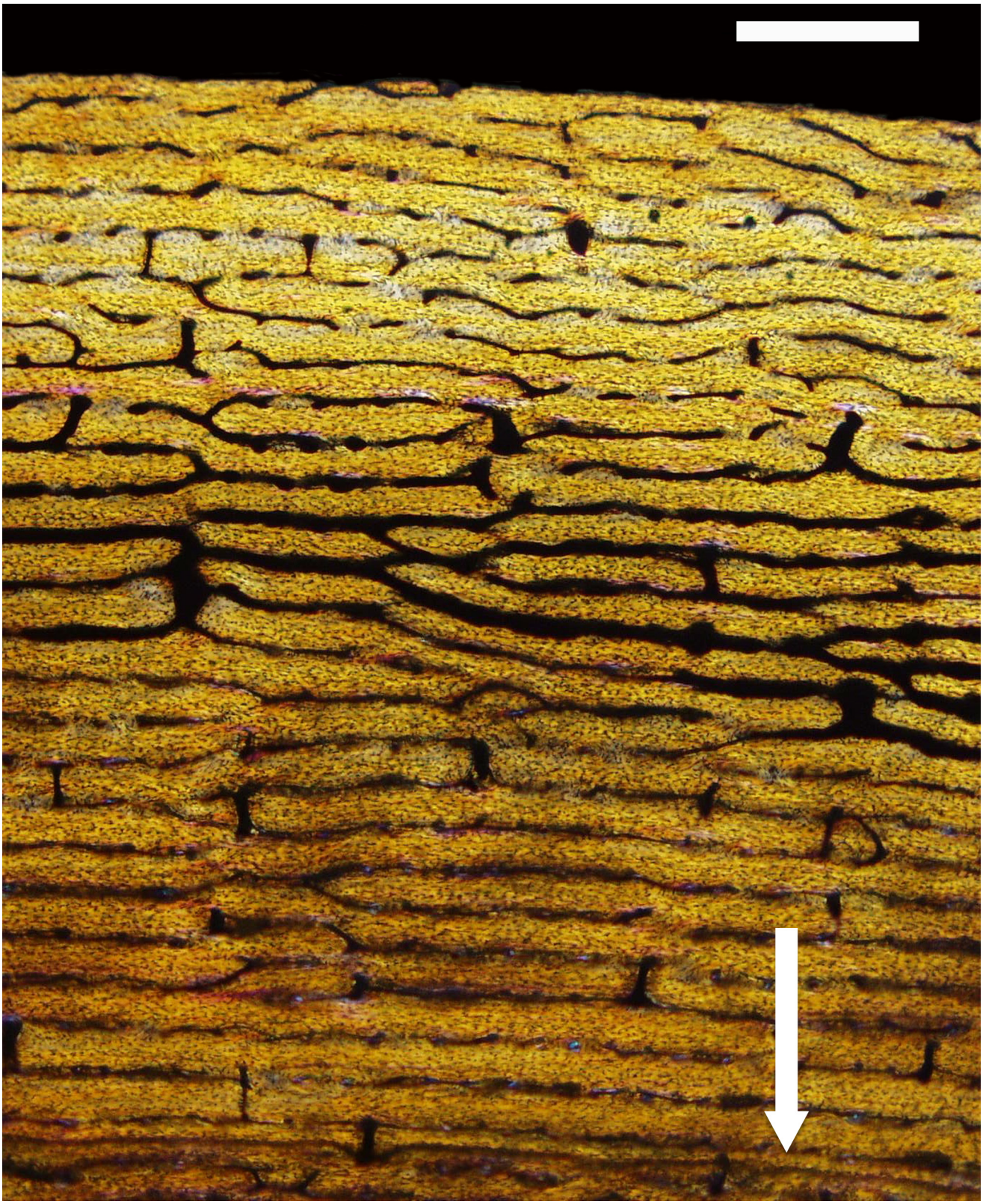

Fig. S2. Diaphyseal stylopodial hindlimb osteohistology of IGM 100/1844. Arrow denote a growth line. Note the incompletely formed primary vascular canals (pitting) at the periosteal border of the element and the broad width of the outermost growth zone element. (Scale bar, 0.5 mm.)

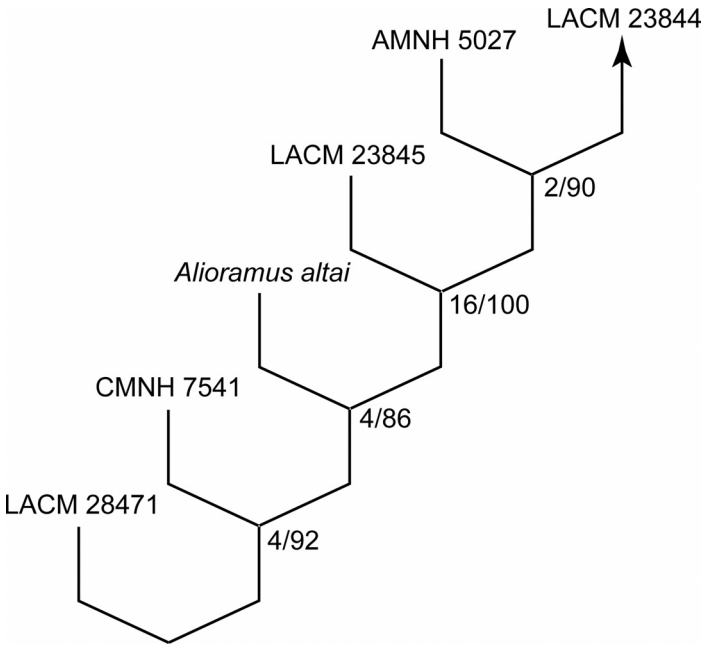

Fig. S3. Single most-parsimonious tree recovered by the ontogenetic analysis (see *Ontogeny Analysis*).

Table S1. Measurements of cranial bones

Bone	Millimeters
Maxilla (left element)	
Anteroposterior length (of ventral margin)	430
Dorsoventral depth (at anterior margin of antorbital fenestra)	120
Anteroposterior length of maxillary antorbital fossa	118
Anteroposterior length of region anterior to antorbital fenestra	225
Nasal (fused left and right elements)	
Anteroposterior length	395
Mediolateral width at the anterior end	50
Mediolateral width at the midpoint	30
Mediolateral width at the posterior end	49
Lacrimal (left element)	
Anteroposterior length of anterior process	130
Dorsoventral depth of ventral process	105
Anteroposterior length of posterior process	27
Jugal (left element)	
Anteroposterior length of entire bone	230
Anteroposterior length of anterior process	111
Dorsoventral depth of anterior process (above antorbital fossa)	32
Anteroposterior length of posterior process	55*
Dorsoventral depth of posteror process (at anterior margin)	27
Dorsoventral depth of dorsal process	90
Postorbital (left element)	
Anteroposterior length of dorsal bar	130
Anteroposterior length of anterior process	45
Anteroposterior length of posterior process	65
Dorsoventral depth of ventral process	80
Squamosal (left element)	
Anteroposterior length of anterior process	70
Dorsoventral depth of anterior process (at midpoint)	35
Long axis length of ventral process	65
Long axis length of medial process	35
Quadratojugal (right element)	
Dorsoventral depth of dorsal process	70
Anteroposterior length of dorsal process (at ventral extent)	23
Dorsoventral depth of anterior process (at posterior extent)	15
Quadrate (left element)	
Dorsoventral depth of shaft (between condyles and head)	110
Anteroposterior length of quadrate flange (perpendicular to shaft)	70
Palatine (right element)	
Anteroposteror length of entire element	225
Dorsoventral depth of waisted region between four processes	25
Ectopterygoid (right element)	
Anteroposterior length	95
Mediolateral width (posterior margin)	40
Epipterygoid (left element)	
Dorsoventral depth	75
Anteroposterior length (at ventral margin)	30
Dentary (left element)	
Anteroposterior length	425
Dorsoventral depth (at third alveolus)	39
Dorsoventral depth (at surangular articulation)	73
Surangular (left element)	
Anteroposterior length	290
Dorsoventral depth (at surangular foramen)	65
Angular (right element)	
Anteroposterior length	204
Dorsoventral depth (maximum)	41
Prearticular (right element)	
Anteroposterior length	285
Splenial (right element)	
Anteroposterior length:	255
Dorsoventral depth (maximum)	62
Supradentary/Coronoid (right element)	
Anteroposterior length	380*

*Incomplete measurement due to breakage.

Table S2. Measurements of the vertebrae (in millimeters)

Specimen Identification	Antero-posterior length of centrum	Minimum transverse width of centrum	Dorso-ventral height of anterior surface of centrum	Medio-lateral width of anterior surface of centrum	Dorso-ventral height of posterior surface of centrum	Medio-lateral width of posterior surface of centrum	Dorso-ventral height of neural spine*	Minimum antero-posterior breadth of neural spine
Cervical 2 (Axis)	36	18	23‡	27‡	33	30	70	21
Cervical 3	42	27	25	35	38	33	?	?
Cervical 4	42	25	35	41	45	?	?	?
Cervical 5	65	27	35	35	37	39†	?	?
Cervical 6	75	35	29‡	43‡	?	?	?	?
Cervical 7	57	36	41	51	46	50	?	?
Cervical 8	60	35	48	59	50	53	?	?
Cervical 9	67	37	44	50	?	65	?	?
Cervical 10	51	35	51	55	56	57	?	?
Dorsal A	55	?	49§	?	55§	?	?	?
Dorsal C	55	26	46	46§	53	50	58	30
Sacral 3	75	26	?	?	?	?	104	51
Sacral 4	79	26	?	?	?	?	101	66
Sacral 5	97	?	?	?	65	46†	93	60
Caudal A	87	32	77	51	75	55	66†	36
Caudal B	82	27	81	55§	83	53	72	37
Caudal C	84	16	37	30	35	37	30	63

Question marks indicate measurements that cannot be made due to breakage and/or poor preservation.
*Measured parallel to the long axis of the spine from the dorsal surface of the transverse processes.
†Minimum measurement due to breakage.
‡Measurement biased by crushing.
§Measurement reconstructed due to breakage.

Table S3. Measurements of pelvic and hind limb bones

Bone	Millimeters
Ilium (right element)	
Depth (dorsoventral) above the acetabulum	160
Depth (dorsoventral) at the posterior end of the postacetabular process	100
Ischium (right element)	
Length (proximodistally)	430
Midshaft width (mediolaterally)	15
Midshaft length (anteroposteriorly)	17
Midshaft circumference	60
Length of obturator process (proximodistally) at midpoint	80
Femur (left element)	
Length (proximodistally)	560
Midshaft width (mediolaterally)	57
Midshaft length (anteroposteriorly)	44
Midshaft Circumference	170
Proximal width	122
Proximal length	44
Distal width	110
Distal length	40

Other Supporting Information Files

SI Appendix